Original Article
Maintaining a regular physical activity aggravates intramuscular tumor growth in an orthotopic liposarcoma model

Mohamad Assi[1], Frédéric Derbré[1], Luz Lefeuvre-Orfila[1], Dany Saligaut[1,4], Nathalie Stock[3], Mickael Ropars[1,2], Amélie Rébillard[1]

[1]EA1274 Laboratory "Movement, Sport and Health Sciences" M2S, University of Rennes 2-ENS Rennes, Bruz 35170, France; [2]Orthopedic and Trauma Surgery Unit-HUGORTHO Pontchaillou University Hospital, Rennes 35033, France; [3]Department of Anatomy and Cytopathology, Pontchaillou University Hospital, Rennes 35033, France; [4]University of Rennes 1, Campus of Villejean, Rennes 35034, France

Abstract: Today, care teams within cancer centers encourage patients to be physically active, after diagnosis, based on data obtained mainly from breast, colon and prostate cancer. Intriguingly, the impact of physical activity (PA) on intramuscular tumors (e.g. sarcomas) has not been specifically addressed and, thus, could be mistakenly confounded with other cancers. In this preclinical study we assessed the impact of PA on intramuscular liposarcoma (LS) evolution. Four-week-old nude male mice were active by voluntary running on wheels, for six weeks. Then, mice were divided into four groups with open or restricted access to wheels, which have received an orthotopic intramuscular injection of either vehicle or human LS, SW872, cells. Active mice presented ~1.5 fold increase in tumor mass, which was mainly due to higher cellular mitosis and proliferation. This bulging intramuscular tumor mass altered muscle function, as evidence by overall muscle strength and maximum running capacity. From a molecular point of view, active mice exhibited poor levels of Phospho-p38$^{Thr180/Tyr182}$ and p21 content in tumors and also displayed low amounts of circulating insulin comparing to inactive counterparts. Insulin induced Phospho-p38$^{Thr180/Tyr182}$ and p21 expression in SW872 cells, *in vitro*. The expression of p21 was regulated in a p38-dependent fashion, since inhibition of p38 activity abolished the up-regulation of p21. Our data suggest that insulin-dependent activation of p38 MAPK-p21 pathway is a possible mechanism responsible for delaying tumor growth in inactive mice. Clinically, patients with lower-extremities LS could be advised to reduce or minimize their levels of PA during the preoperative period.

Keywords: Physical activity, cancer, insulin, p38 MAPK, p21

Introduction

Physical activity (PA) is an adjuvant strategy that could be prescribed for cancer patients before, during and after conventional anticancer treatments to manage secondary symptoms, preserve muscle strength, allow hard treatments to go forward and optimize recovery [1]. A body of evidence indicates that PA can reduce about 25% the risk of colon and breast cancer, with possible evidence in prostate, lung and ovary cancer [1-3]. Interestingly, PA also appears to delay disease recurrence, highlighting a possible role in the suppression of tumor growth [4-6]. To date, 64% of preclinical exercise-oncology studies are likely to support a positive effect of PA on tumor incidence, growth or progression, regardless the type/localization of tumor and modality/intensity of PA [7]. Intriguingly, the majority of these studies were performed on animals bearing subcutaneous malignancy, in order to monitor tumor growth kinetics; whereas only few reports have used orthotopic models and none have lend attention to the impact of PA on intramuscular tumors [7].

Liposarcoma (LS) is the most frequent type of soft tissue sarcoma (20%) that arises from adipocytes and fibroblasts located within deep

soft tissue [8]. It is most commonly found within thighs of patients [9]. This particular localization inside skeletal muscle constitutes an awkward mass that may impede the capacity of muscle to produce sufficient force and ensure basic physical needs. Indeed, survivors of lower-extremities sarcoma exhibit physical quality deterioration and are unlikely to meet PA guidelines [10]. However, the impact of PA on intramuscular tumors and related muscle dysfunction still poorly understood; thus, there is no recommendation about the levels of PA to advise for patients with lower-extremities sarcomas before any treatment (e.g. surgery, chemotherapy and radiotherapy).

Exercise-oncology remains a field with several unexplored areas and little is known about the exact molecular mechanisms through which exercise could induce its protective effects. However, it is thought that exercise-mediated changes in systemic inflammation, hormones, angiogenesis, redox status, immune system and insulin sensitivity could impact signaling pathways involved in tumor growth/progression [11]. In this light, mitogen-activated protein kinase (MAPK) family members constitute a major target. Indeed, it has been suggested that PA could modulate tumor growth *via* the regulation of MAPK pathways [12], which in turn control the expression and stabilization of a large number of cell cycle activators/inhibitors [13]. Nonetheless, as each tumor type possesses specific characteristics, molecular pathways mobilized in response to PA may also differ [14, 15]. For example, in response to the same modality of PA, tumors "inside-muscle" could behave differently compared to those located "outside-muscle". In the present work, we were interested to study the usefulness of PA in the context of a direct tumor-skeletal muscle interaction. We addressed for the first time the impact of regular PA on intramuscular LS growth from a molecular point of view.

Materials and methods

Ethics approval and study design

All procedures described below were performed in accordance with the recommendations of European community (directive 2010/63/EU) and were approved by the French ministry of higher education and research, in accordance with the local committee of research ethics of Rennes (authorization no. APAFS#581-2015050411405743). Four-week-old nude male mice were obtained from Harlan (Rossdorf, Germany) and housed in the animal care facility of the laboratory "Movement, Sport and health Sciences" (agreement no. A35-047-34). During the first six weeks, all mice (n = 36) performed voluntary running on activity wheels (Intellibio, France) placed individually in their cages. Wheels were connected to counters that recorded the daily performed distance by each mouse. Before inoculation, mice were homogeneously assigned into four groups (n = 9/group) based on PA levels, during the last six weeks. Then animals have received an intramuscular injection of either liposarcoma SW872 cells or DMEM alone (vehicle). Activity wheels were blocked the day of injection for inactive control (CTLI) and liposarcoma (LSI) mice, whereas active control (CTLA) and liposarcoma (LSA) mice maintained PA until the end of the protocol (**Figure 1A**). At eight weeks post-injection (PI), all animals were anesthetized with Ketamine-Xylazine cocktail and sacrificed. Tumors, peri-tumoral tissues, lungs and skeletal muscles were weighted and immediately frozen in liquid nitrogen or fixed in 4% paraformaldehyde (PFA). Blood was obtained by intra-cardiac puncture, either immediately used to perform hematocrit and hemoglobin measures or placed in EDTA-coated tubes for plasma collection.

Survival curve

A survival curve protocol was performed on four-week-old nude mice (n = 20) to determine whether or not PA affect the lifespan of mice bearing SW872 tumor. The same experimental procedure used previously was repeated, namely, all mice were physically active for six weeks. Next, mice were randomized into two groups (n = 10/group) and then received an intramuscular injection of SW872 cells. For the LSA group, mice maintained activity on wheels, whereas for LSI the wheels were blocked the day of injection. The survival protocol lasted six months after inoculation and was ended when all mice died.

Liposarcoma cell line SW872 and intramuscular injection

Human SW872 cells (passage 27) were obtained from Cell Line Services (CLS; Germany).
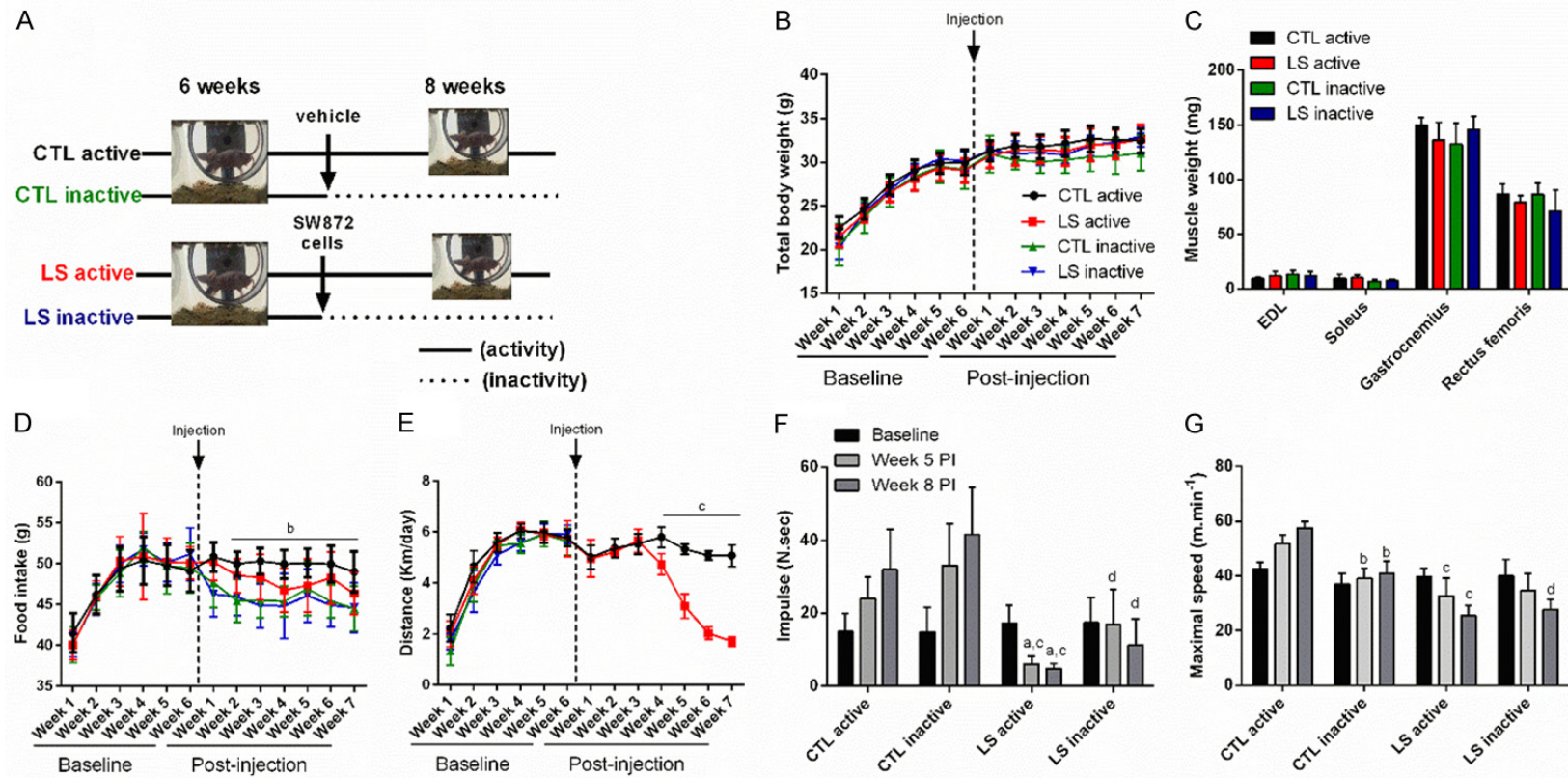
Figure 1. The impact of LS and/or PA levels on anthropometric parameters. (A) Experimental design of the present study. (B) The weight of total body and (C) different skeletal muscles measured at the end of the protocol. (D) Food intake recorded once a week at the baseline and twice weekly PI. (E) Week average of voluntary running distance per group, values were registered daily and results expressed in (Km/day). (F) Impulse score reflecting overall muscle strength and (G) maximal speed test to evaluate running endurance capacity, were performed at the baseline and five and eight weeks PI. Results are expressed as mean ± SEM (CTLA: n = 9; CTLI: n = 8; LSA: n = 9; LSI: n = 8); (a) LSA vs. LSI, (b) CTLA vs. CTLI, (c) CTLA vs. LSA, (d) CTLI vs. LSI. Statistical difference between the four groups in (B-D, F and G) was tested using a two-way ANOVA with Tukey's post hoc test. A student t-test was performed for comparison between two groups in (E). Results were considered significant at $P < 0.05$.

Table 1. List of primers used for RTqPCR analysis

	Gene (Human)	Forward (5'→3')	Reverse (5'→3')
Cell cycle	CDC25A	GCAACCACTGGAGGTGAAGA	CCAACAGCTTCTGAGGTAGGG
	CDC25C	GAGGAACCCCAAAACGTTGC	TCTATGGCCACGGTCCAAAC
	PLK-1	GGATGTGTGGTCCATTGGGT	GCAGCTCGTTAATGGTTGGG
	p14	CGAGTGAGGGTTTTCGTGGTTC	CACGGGTCGGGTGAGAGTG
	p16	TCGGCTGACTGGCTGG	GTGAGAGTGGCGGGGTC
	p21	AGTCAGTTCCTTGTGGAGCC	CATTAGCGCATCACAGTCGC
	p27	GCCTCAGAAGACGTCAAACG	TCCAACGCTTTTAGAGGCAGA
	CyclinD	GATGCCAACCTCCTCAACGA	GGAAGCGGTCCAGGTAGTTC
	CyclinE	CCCCATCATGCCGAGGGAG	TGTCAGGTGTGGGGATCAGG
Inflammation	IL1β	CAGAAGTACCTGAGCTCGCC	AGATTCGTAGCTGGATGCCG
	IL6	AGTGAGGAACAAGCCAGAGC	AGCTGCGCAGAATGAGATGA
	IL10	TACGGCGCTGTCATCGATTT	TAGAGTCGCCACCCTGATGT
	TNFα	CTCTTCTGCCTGCTGCACT	CTCTCAGCTCCACGCCATT
	TGFβ	ACAGCAACAATTCCTGGCGA	GGTAGTGAACCCGTTGATGTCC
	MCP1	CTCGCCTCCAGCATGAAAGT	AGATCTCCTTGGCCACAATGG
Antioxidant enzymes	SOD1	TGAAGGTGTGGGGAAGCATT	AGTCTCCAACATGCCTCTCTTC
	SOD2	CGGCATCAGCGGTAGCA	CAGTGCAGGCTGAAGAGCTA
	CAT	TAACGTTACTCAGGTGCGGG	AGATCCGGACTGCACAAAGG
	Gpx2	GACTTCACCCAGCTCAACGA	ATGCTCGTTCTGCCCATTCA
Angiogenesis	VEGF	CATCACCATGCAGATTATGCGG	GAGGCTCCAGGGCATTAGAC
	ANGPT1	CGTGGAGCCGGATTTCTCTT	TTAGTACCTGGGTCTCAACATCTG
	ANGPT2	CAAACTCAGCTAAGGACCCCA	CCATCCTCACGTCGCTGAAT
	PDGFA	TCCGTAGGGAGTGAGGATTC	TCGTAAATGACCGTCCTGGT
	PDGFB	CTACCTGCGTCTGGTCAGC	CCCCATCTTCCTCTCCGGG
House Keeping Genes	RPLO4	TTCCTTTTCCTGTGGCAGCA	TTTTGCCAGATGACTCCCCC
	HPRT1	GGCGAACCTCTCGGCTTT	CACCCTTTCCAAATCCTCAGC

Authenticity was verified by CLS using STR DNA profiling. Cells were maintained in a humidified atmosphere at 37°C; 5% CO_2 and cultured in DMEM supplemented with 2 mM L-glutamine, 10% fetal bovine serum (FBS) heat inactivated, together with penicillin 100 µg/ml and streptomycin 100 U/ml. The day of injection, SW872 cells were pelleted after centrifugation (500 g for 6 min at 25°C) and then taken up with DMEM. Mice have received an intramuscular inoculation of either SW872 cells ($2 × 10^6$ cells in 100 µl; passage 32) or vehicle, at the inner side of the right hindlimb to insure that the volume was injected within skeletal muscle but not subcutaneously or in the fascia. Body weight and food intake were monitored weekly at the beginning of the protocol and then twice per week when tumors started to appear.

Grip strength and maximal speed test

Muscle strength was determined by performing a wire hang test at the baseline and five and eight weeks PI. The test was performed for each mouse by the same experimenter to avoid operator-dependent variability. Mice were placed on the grid, then brought to cling on the wire by gently stirring. Next, the grid was inverted and the time of animal gripping was recorded three consecutive times separated by 20 min of rest. The best time of latency was retained and normalized to mouse weight in order to determine the holding impulse [16, 17]. A maximal speed test was performed, at the baseline and five and eight weeks PI, on a treadmill placed on a flat angle (slope 0%). The test began with 5 min warm-up (12 m/min) and then the speed increased progressively by 2 m/min every 2 min until exhaustion.

Histological analysis

Tumor and lung tissues were fixed with PFA for 24 h and embedded in paraffin. Tissue sections of 4 µm thickness were obtained using LEICA microtome and mounted on glass slides.

Tumor sections were stained with: Hematoxylin & Eosin (H&E) for histopathology analysis, CD31 to assess blood vessels density and Ki-67 to determine the proliferating rate of tumor cells. Lungs were scrutinized for metastatic tumor nodules by performing serial sections. Three sections of 4 μm separated each other by a distance of 40 μm were made per lung and stained with H&E. The number of metastatic tumor nodules in lungs was counted by observing slides on a two-headed optical microscope. Sections were analyzed to determine the metastatic area using the NDP image software.

RNA extraction and RT-qPCR

Tissues were grinded in liquid nitrogen and the obtained powder was used to perform experiments. Total RNA was extracted using Trizol® reagent according to the manufacturer's protocol (Sigma Aldrich). RNA amounts were determined by NanoDrop spectrophotometer and RNA quality was controlled on 1.2% agarose gel using the FlashGel electrophoresis system (Lonza). Reverse transcription reaction (RT) was carried out on 1 μg of total RNA (IScript reverse transcription, 170-8840). Then Sybergreen real-time PCR experiments were performed on RT products in a final volume of 10 μl containing: 5 μl of cDNA (diluted at 1/5), 0.2 μl of primers (10 μM) and 4.8 μl of SYBR® Green Supermix (1725271, Biorad). Experiments were monitored in CFX Real-Time machine (Biorad). The expression of target genes was normalized to reference genes and the relative expression was calculated using the ΔΔCt method on CFX-Manager software. Used primers are listed in **Table 1**.

Immunoblotting analysis

Tissues were grinded in liquid nitrogen and the obtained powder was used to perform experiments. Samples were lysed and immunoblot experiments were performed as described previously [17]. The following primary antibodies were used: anti-Hsc70 (sc-7298, Santa-Cruz), anti-Phospho ERK1/2$^{Thr202/Tyr204}$ (4370S, Cell Signaling Technologies), anti-ERK total (sc-292838, Santa-Cruz), anti-phospho JNK$^{Thr183/Tyr185}$ (sc-6254, Santa-Cruz), anti-JNK total (sc-7354, Santa-Cruz), anti-phospho p38$^{Thr180/Tyr182}$ (9211S, Cell Signaling Technologies), anti-p38 total (9212S, Cell Signaling Technologies), anti-p21$^{Waf1/Cip1}$ (2947S, Cell Signaling Technolo-

gies), anti-p27 (2552S, Cell Signaling Technologies), anti-Phospho p53^{ser15} (9284S, Cell Signaling Technologies), anti-p53 total (9282S, Cell Signaling Technologies), anti-cleaved caspase-3 (9664S, Cell Signaling Technologies), anti-Bax (2772, Cell Signaling Technologies) and anti-Bcl2 (2870, Cell Signaling Technologies). Densitometry analysis was performed using Image Gauge v 4.0 software.

Enzyme-linked immunosorbent assay (ELISA)

The levels of circulating IL-6 (431307, BioLegend) and insulin (EZRMI-13K, Millipore) were measured in plasma of non-fasted tumor-bearing mice. For TNF-α, total proteins were extracted from peritumoral tissues and then TNF-α concentrations were measured using a specific ELISA kit (430907, Biolegend). Briefly, 20-50 μl of peritumoral protein lysate or plasma were added to each well pre-coated with the appropriate primary antibody. After incubation with a detection antibody, substrate solution was added to the plate and a blue color developed proportionally with the levels of protein in question. Optical density (OD) was measured at 450 nm respectively using a microplate reader.

4-Hydroxynonenal-protein adducts analysis

Proteins (50 μg) from tumor extracts were charged on 12.5% SDS-Acrylamide gel. After transfer, PVDF membranes were incubated for 15 min at room temperature (R-T) with a solution of 250 mM sodium borohydride and 100 mM MOPS. Membranes were incubated, overnight at 4°C, with a primary antibody that binds to HNE modified proteins (ab46545, Abcam). The next day, membranes were washed with PBST (Phosphate Buffered Saline/0.05% Tween-20) and incubated with secondary antibody for 1 h at R-T. Finally, membranes were scanned using the Odyssey imaging system.

Insulin treatment and p38 MAPK inhibition in vitro

SW872 cells were seeded at a density of 300 × 10^3 cells/well in a six-well plate, incubated overnight and, then exposed to 100 nM of insulin (I6634-50MG, Sigma Aldrich) at different time points (5, 10 and 30 min; 1, 2 and 4 h). Phosphorylated levels of p38 and p21 protein content as well as the expression of p21 at the

mRNA level were assessed by immunoblotting and RTqPCR, respectively, as previously described. For p38 inhibition experiments, SW872 cells were pre-treated for 2 h with 10 µM of SB203580 (5633, Cell Signaling), a well-known specific inhibitor for p38 activity. Then, cells were treated with insulin for 1, 2 and 4 h to perform RTqPCR analysis and for 4 h to perform immunoblotting experiments.

Statistical analysis

Median-survival was determined by the Kaplan-Meier method and analyzed by the log-rank test. Data were presented as mean ± SEM. Normality and equal variance were tested before statistical analysis. For body weight, food intake, impulse and maximal speed, a two way ANOVA test was used to compare all four groups. Further interactions were analyzed with a Fisher LSD test. When data did not follow a normal distribution, logarithmic (log) values were calculated and then a two way ANOVA was performed on log function. Significant difference between two groups was examined by a student *t*-test for tumor, lung and peritumoral tissues. A non-parametric Mann-Whitney rank sum test was used instead of *t*-test, when data failed to pass the normality test. Results were considered statistically different at $P < 0.05$.

Results

*Physical activity exacerbated skeletal muscle dysfunction in mice bearing SW872 tumor*

As mice can develop a number of common clinical conditions in response to cancer, we firstly assessed how the progressive growth of LS tumor can influence mice's overall health. At baseline, total body weight, food intake and daily PA levels were similar between all experimental groups. At end of protocol, total body and skeletal muscle weights did not significantly change between different conditions (**Figure 1B** and **1C**). LS tumor did not induce neither anorexia nor anemia, since chow consumption (**Figure 1D**), hematocrit and hemoglobin levels did not differ between cancer and control groups (data not shown). Food intake was mainly reduced in inactive mice, after the wheel lock. This effect was only significantly different between CTLA and CTLI mice starting from the 2th week PI (49.98 ± 1.46 vs. 45.42 ± 2.59 g,

$P < 0.001$; **Figure 1D**). Daily PA levels started to progressively decrease starting from the 4th week PI until the end of the protocol in LSA mice, while the CTLA group preserved the same pace throughout the protocol (5.08 ± 0.41 vs. 1.71 ± 0.19 km/day, $P < 0.001$; **Figure 1E**). Given the location of tumor within skeletal muscle, we determined the impact of tumor on muscle at different time points. At baseline, all mice exhibited the same level of muscle performance as indicated by impulse and endurance running capacity. Impulse test showed that overall muscle strength in tumor-bearing mice was inferior to control. Unexpectedly, impulse score was dramatically reduced, at 5 weeks PI, in LSA compared to LSI mice (6.08 ± 2.12 vs. 16.82 ± 9.64 N.sec, $P < 0.001$; **Figure 1F**). At 8 weeks PI, muscle strength deceased further in both LSA and LSI, but remained considerably higher in the latter (4.89 ± 1.28 vs. 11.22 ± 7.28 N.sec, $P < 0.001$; **Figure 1F**). Endurance running capacity increased in CTLA but not in CTLI, at 5 and 8 weeks PI. On the other hand, this parameter was considerably diminished at 5 weeks PI only in LSA and at 8 weeks PI in LSA and LSI comparing to CTLA and CTLI, respectively. Importantly, the reduction was more pronounced in LSA than LSI when referring to their respective controls (CTLA vs. LSA: 57.5 ± 2.5 vs. 25.5 ± 3.5 m.min^{-1} and CTLI vs. LSI: 41 ± 4.5 vs. 27.71 ± 3.75 m.min^{-1}, $P < 0.001$; **Figure 1G**). Our findings strongly indicate that intramuscular SW872 tumor reduced both muscle strength and endurance capacity in mice and that maintaining a steady PA level aggravated this phenomenon.

*Active mice exhibited an increased intramuscular tumor growth*

Since the musculoskeletal function was seriously altered in active tumor-bearing mice, we wondered that a change in the intramuscular tumor mass may be partly responsible; thus, we focused the next part to study the impact of PA on tumor growth. Unexpectedly, tumors in LSA mice were, visibly, much bigger than in LSI mice (**Figure 2A**). We found that average tumor weight of LSA mice was superior to the inactive group (3.55 ± 0.89 vs. 2.24 ± 0.99 g, $P = 0.03$; **Figure 2B**). Histopathology analysis on tumor sections revealed that both groups have developed an undifferentiated grade-3 LS (**Figure 2C**). However, mitotic count was elevated in tumor of active animals (38.44 ± 9.97 vs.
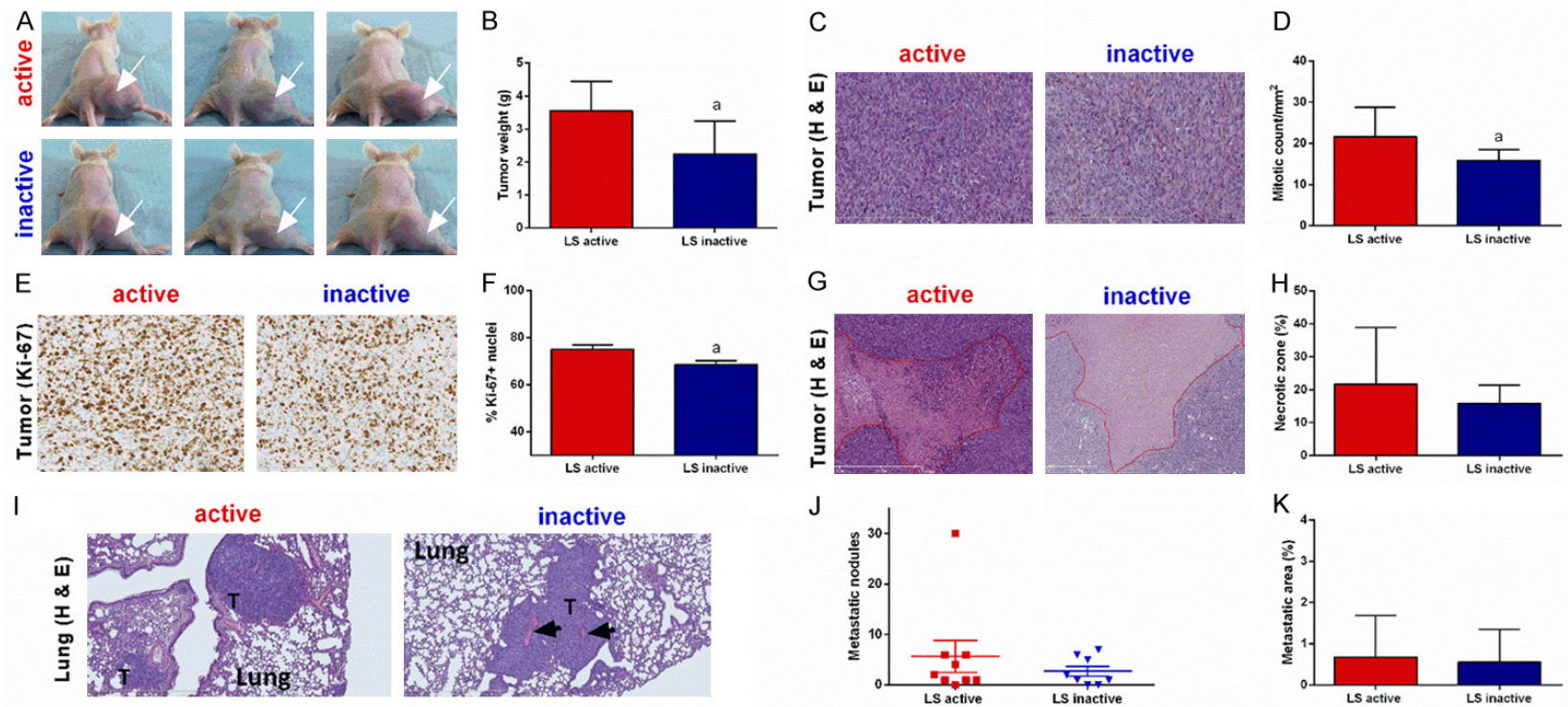
Figure 2. PA modulated intramuscular LS tumor growth. (A) Photos showing difference in intramuscular tumor size between active and inactive mice. (B) Average tumor weight at eight weeks PI. (C) Tumor sections stained with H&E (view 200 ×) showing undifferentiated tumor cell architecture and cells undergoing mitosis. (D) Mitotic count obtained from tumor sections presented in (C). Ten distinct fields were counted per tumor section using a two-headed microscope and results were expressed as (mitotic count/mm^2). (E) Tumor sections stained with DAPI (bleu) and Ki-67 (brown) (view 200 ×). One tumor section per mouse was performed in the wider part of the tissue. (F) For each section, the number of Ki-67 positive cells was counted in five distinct field and normalized to the total number of nuclei, in order to determine the percentage of proliferating cells. (G) Tumor sections stained with H&E (view 50 ×). Necrotic zones were delimited with a red line. (H) Percentage of tumor necrotic zones per total tumor area. (I) Lung sections stained with H&E (view 50 ×). Metastatic tumor nodules were mainly found around blood vessels (black arrow) and indicated with the letter "T". (J) The total number of metastatic tumor nodules. (K) The percentage of metastatic zone per total lung area. Results are expressed as mean ± SEM (LSA: n = 9; LSI: n = 8); (a) LSA vs. LSI. Statistical difference between LSA and LSI was tested with a student t-test. Results were considered significant at $P < 0.05$.
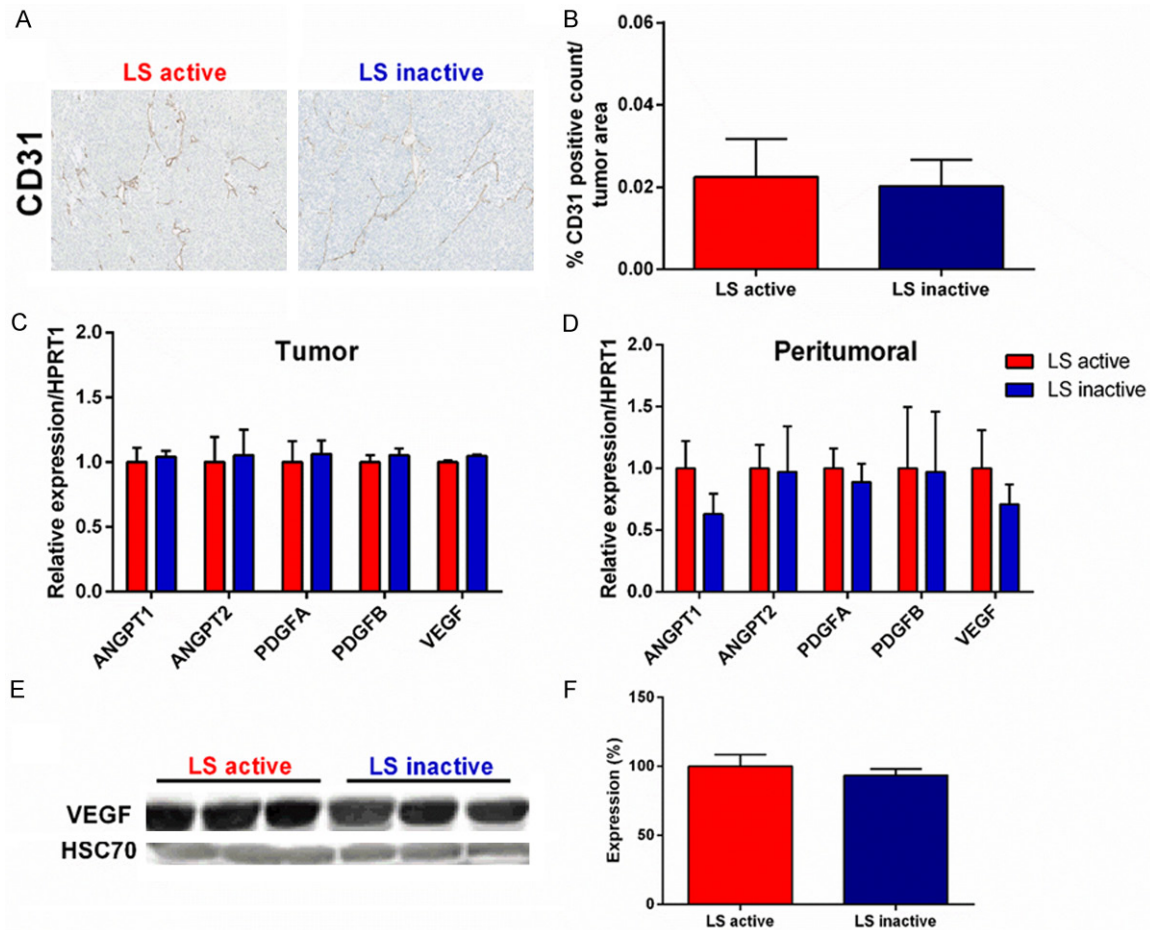
Figure 3. PA did not affect angiogenesis markers. (A) Tumor sections stained with DAPI (bleu) and CD31 (brown) a marker of blood vessels density (view 100 ×). (B) Percentage of CD31 positive zones per total tumor area. Transcripts levels of angiogenesis-related genes in (C) tumor and (D) peritumoral environment, assessed by RTqPCR analysis. (E) Immunobloting analysis for VEGF protein content in tumor extracts. (F) Densitometry quantification for VEGF. Results are expressed as mean ± SEM (LSA: n = 9; LSI: n = 8). Statistical difference between LSA and LSI was tested with a student *t*-test.

25.36 ± 7.26 mitosis/mm², *P* = 0.04; **Figure 2D**) and coincided with an increase in proliferation rate, as assessed by Ki-67 staining (75.02 ± 4.1 vs. 68.49 ± 3.3%, *P* = 0.018; **Figure 2E and 2F**). Necrosis is a factor that could promote tumor growth in a certain number of cancers [18]. However, the percentage of necrotic zones within tumor tended to increase in the active group but did not reach any statistical difference (**Figure 2G and 2H**). Additionally, both groups developed a low level of pulmonary metastasis (**Figure 2J and 2K**). Tumor nodules within lungs were principally localized surrounding blood vessels (Arrow; **Figure 2I**). Similarly, the density of blood vessels as assessed by CD31 staining on tumor sections was comparable in active and inactive mice

(**Figure 3A** and **3B**). The mRNA expression of angiogenesis genes such as vascular endothelial growth factor (*VEGF*) remained unchanged in tumor and peritumoral environment of both LSA and LSI mice (**Figure 3C** and **3D**). In line with the enhanced tumor growth in active mice, these animals seemed to develop an advanced stage of disease compared to their inactive counterparts, as only LSA mice exhibited significant loss of visceral adipose tissue mass, which was negatively correlated with tumor weight (r = -0.74; *P* < 0.001; **Figure 4A** and **4B**). These results indicate that mice maintaining voluntary running exhibited greater intramuscular SW872 tumors and manifested early cachexia events, without any change in intra-tumor vascularization and lung metastasis.
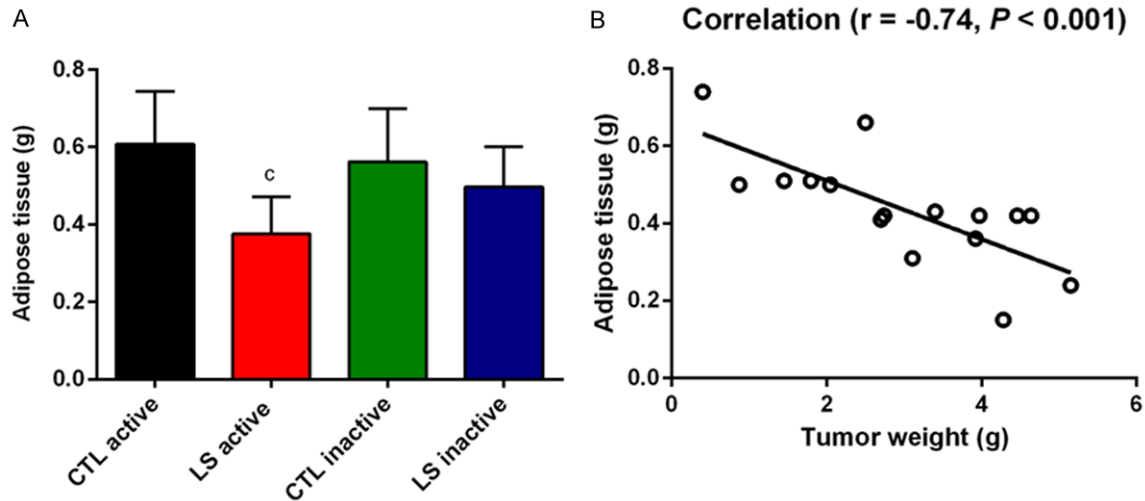
Figure 4. Negative correlation between visceral adipose tissue mass and tumor weight. (A) Visceral adipose tissue mass weighed at end of protocol. Statistical difference between groups was tested using two-way ANOVA with Tukey's post hoc test. Results are expressed as mean ± SEM (CTLA: n = 9; CTLI: n = 8; LSA: n = 9; LSI: n = 8); (c) CTLA vs. LSA. Results were considered significant at $P < 0.05$. (B) Pearson's correlation, showing a negative relationship between adipose tissue mass and tumor weight in both LSA and LSI mice.

*Tumors of active mice displayed poor p38 MAPK phosphorylation and p21 expression*

Based on our results, it seems that proliferation is the main mechanism through which PA modulated the growth of LS tumors. Our finding that apoptosis markers were unchanged in tumors of both groups, as evidenced by similar content of cleaved caspase-3, Bax and Bcl-2, may also support this point of view (**Figure 5F** and **5G**). We analyzed the mRNA expression of numerous well-known cell cycle-related genes. Only the expression of the cell cycle inhibitor *p21*, but not that of *p27*, *p16^INK4^* and *p14^ARF^*, was 2-fold higher in tumors of LSI mice compared to LSA (1 ± 0.35 vs. 2.04 ± 0.5, $P = 0.02$; **Figure 5A**). Accordingly, the protein content of p21, but not that of p27, p53 and Phospho-p53^ser15^, was significantly elevated in LSI tumors (+46.77%, $P = 0.015$; **Figure 5B** and **5C**). Activated MAPK proteins regulate the expression of cell cycle genes and have been described previously to play an important part in both tumor progression and suppression [13]. Thus, we assessed the phosphorylation status (activation) of the three main MAPKs, ERK1/2, JNK and p38. The phosphorylation of ERK1/2^Thr202/Tyr204^ and JNK^Thr183/Tyr185^ was fluctuating inter/intra-group and did not significantly differ between LSA and LSI (**Figure 5D** and **5E**). Interestingly, the levels of Phospho-p38^Thr180/Tyr182^ were dramatically higher in tumors of LSI mice compared to LSA (+86.05%, $P = 0.02$; **Figure 5D** and **5E**). Together, these data indicate that p38 MAPK was activated in tumor of inactive mice and coincided with higher p21 expression at both transcriptional and protein level.

Physically active SW872 mice showed lower levels of circulating insulin

In a first step, we wanted to determine which stimuli could be potentially responsible for the activation of p38. The induction of p38 may be sensitive to a number of factors including inflammation, oxidative stress, inflammation and DNA damage [19-21]. Seemingly, intra-tumor oxidative damage, antioxidant defense and DNA damage signatures were not modulated by PA, as evidenced by the content of HNE-protein adducts (marker of oxidative damage) (**Figure 6A** and **6B**), mRNA expression of antioxidant genes (i.e. *CAT*, *SOD1/2* and *GPX2*) (**Figure 6C**) and content of γH2AX (marker of DNA damage) (**Figure 6D** and **6E**). Additionally, PA did not modulate local inflammation in tumor and peritumoral environment, since the expression of pro and anti-inflammatory cytokines (i.e. *IL-1β, IL-6, IL-10, TNF-α, TGF-β* and *MCP-1*) was similar in LSI and LSA animals (**Figure 6F-H**). In the same way, systemic inflam-
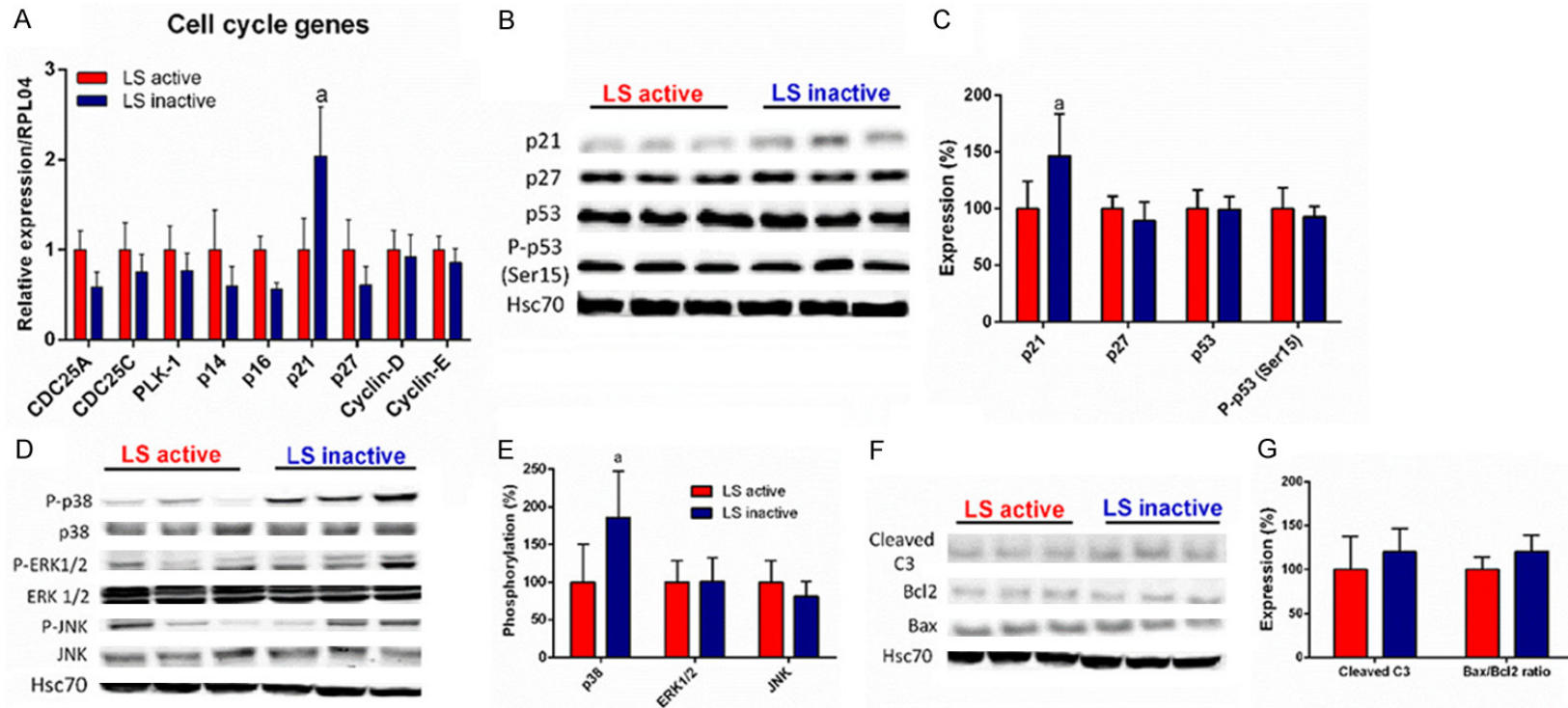
Figure 5. PA affected signaling pathways regulating proliferation. (A) Relative expression of cell cycle genes in tumors of LSA and LSI mice, determined by RTqPCR. (B) Immunoblot analysis of p21, p27, p53 and Phospsho-p53^{ser15} protein content. (C) Densitometry analysis for blots presented in (B). (D) Immunoblot analysis for Phospho-p38$^{Thr180/Tyr182}$, Phospho-ERK1/2$^{Thr202/Tyr204}$ and Phospho-JNK$^{Thr183/Tyr185}$ and their respective total protein form. (E) Densitometry analysis showing the ratio "Phosphorylated: total form" for p38, ERK1/2 and JNK. (F) Immunoblot analysis for cleaved caspase-3, Bax and Bcl-2 protein content. (G) Densitometry analysis corresponding to the blots showed in (F). All these experiments were performed on tumor extracts. Hsc70 was used as a load control. Results are expressed as mean ± SEM (LSA: n = 9; LSI: n = 8); (a) LSA vs. LSI. Statistical difference between LSA and LSI was tested with a student t-test. Results were considered significant at $P < 0.05$.
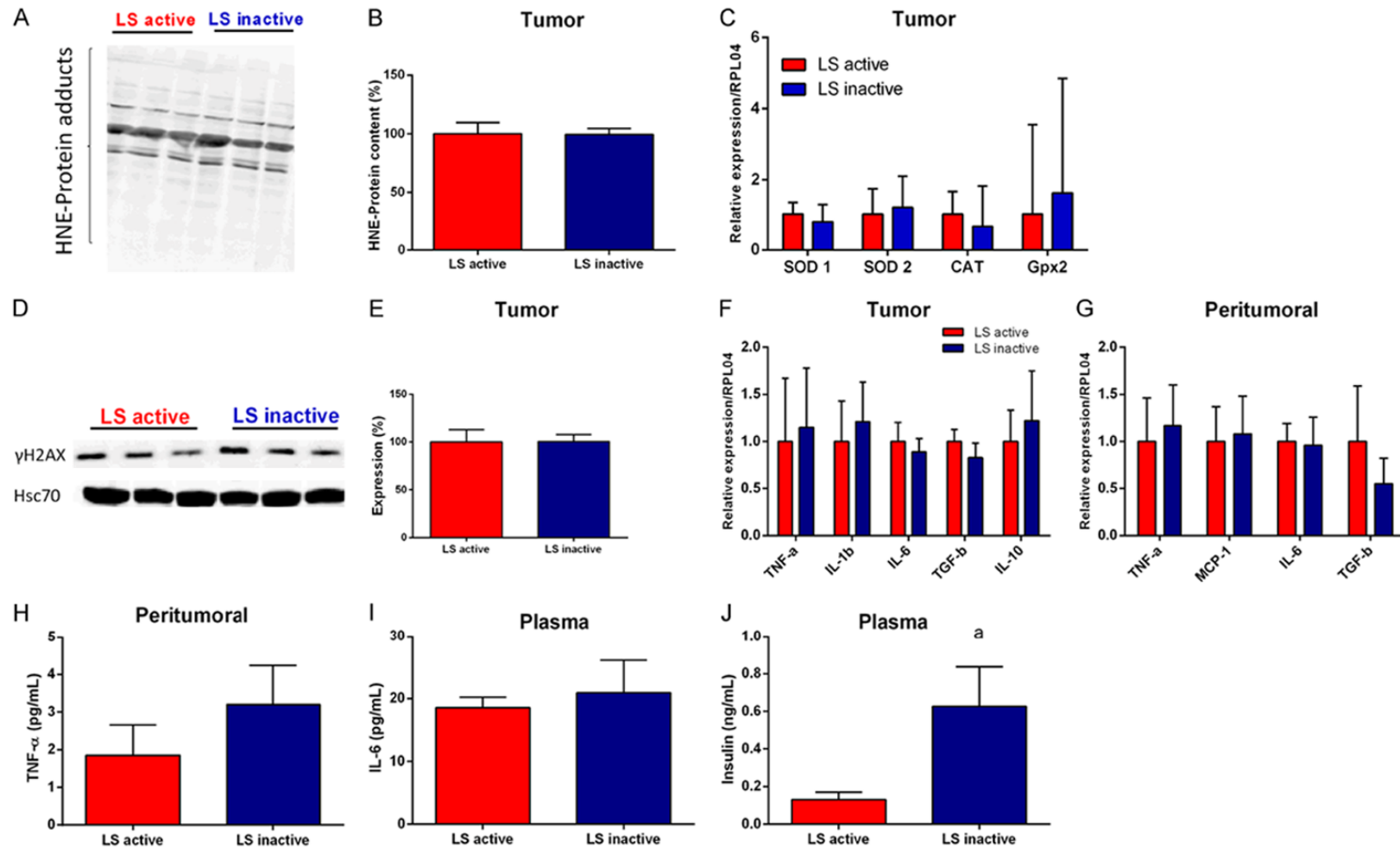
Figure 6. Modulation of circulating insulin rates in tumor-bearing mice according to the level of PA. (A) Immunoblot showing tumor content of HNE-protein adduct, an indicator of lipid peroxidation. (B) Densitometry analysis for HNE-protein adducts. (C) Relative expression of antioxidant genes in tumor, measured by RTqPCR. (D) Immunoblot analysis for the DNA damage marker, γH2AX, in tumor extracts. (E) Densitometry quantification corresponding to γH2AX. Transcripts levels of inflammatory genes in (F) tumor and (G) peritumoral environment assessed by RTqPCR. (H) Amounts of protein TNF-α (pg/mL) in peritumoral tissue, measured using a specific ELISA kit. Circulating levels of (I) IL-6 (pg/mL) and (J) insulin (ng/mL) in plasma samples of mice in non-fasting state, determined by specific ELISA kits. Hsc70 was used as a load control. Results are expressed as mean ± SEM (LSA: n = 9; LSI: n = 8); (a) LSA vs. LSI. Statistical difference between LSA and LSI was tested with a student t-test. Results were considered significant at $P < 0.05$.
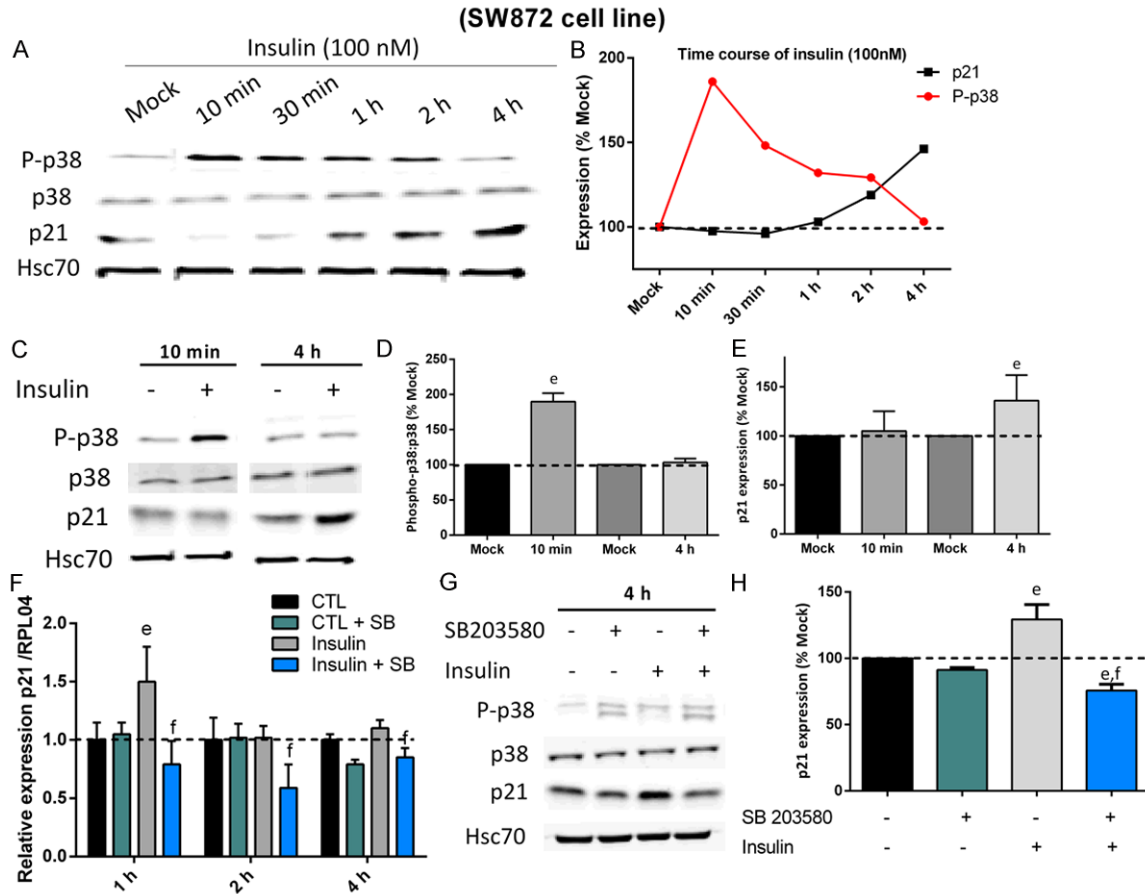
Figure 7. Regulation of p21 expression by p38 MAPK in response to insulin treatment *in vitro*. (A) Changes in p38$^{Thr180/Tyr182}$ phosphorylation and p21 expression over time in SW872 cells exposed to insulin. (B) Densitometry analysis corresponding to blots presented in (A) (n = 2). (C) Immunoblot analysis for p38$^{Thr180/Tyr182}$ phosphorylation and p21 expression at 10 min and 4 h of insulin treatment. Densitometry quantification showing (D) the ratio of "Phosphorylated: total form" of p38 (n = 4) and (E) p21 expression (n = 4). (F) RTqPCR analysis for p21 mRNA expression at 1, 2 and 4 h of insulin treatment, in the presence or absence of SB203580 (n = 3). (G) Immunoblot analysis for p38$^{Thr180/Tyr182}$ phosphorylation and p21 expression at 4 h of insulin treatment, in the presence or not of SB203580. (H) Densitometry quantification for p21 expression (n = 3). Hsc70 was used as a load control. (A, B) Experiments were performed two times from two independent cell culture. (C-H) All experiments were performed at least three times from three independent cell culture. Results are expressed as mean ± SEM; (e) Mock vs. insulin-treated, (f) Insulin-treated without SB vs. insulin-treated with SB. (C-E) Statistical difference was tested with a student *t*-test. (F-H) Statistical difference was tested using a two-way ANOVA with Tukey's post hoc test. Results were considered significant at *P* < 0.05.

mation as evidenced by the amounts of circulating IL-6 was comparable in active and inactive tumor-bearing animals (**Figure 6I**). As PA is a key regulator of insulin sensitivity [22], we measured the circulating levels of insulin, and reported a ~4-fold increase in samples of inactive animals (0.14 ± 0.03 vs. 0.62 ± 0.2 ng/mL, *P* = 0.028; **Figure 6J**). These compelling evidences may suggest the existence of an interrelationship between the increase in circulating insulin levels, activation of p38 MAPK and high p21 expression in the tumors of inactive mice.

Insulin induced p38 MAPK-dependent p21 expression in SW872 cells

We next aimed to verify whether or not insulin could induce p38 activation and p21 expression. In SW872 human LS cells, insulin induced phosphorylation of p38$^{Thr180/Tyr182}$ with a peak observed at 10 min post-treatment (PT) (+ 89%, *P* = 0.01; **Figure 7C** and **7D**). Then, phosphorylated levels of p38$^{Thr180/Tyr182}$ decreased progressively and returned to levels comparable to those of control at 4 h PT (**Figure 7A** and **7B**).
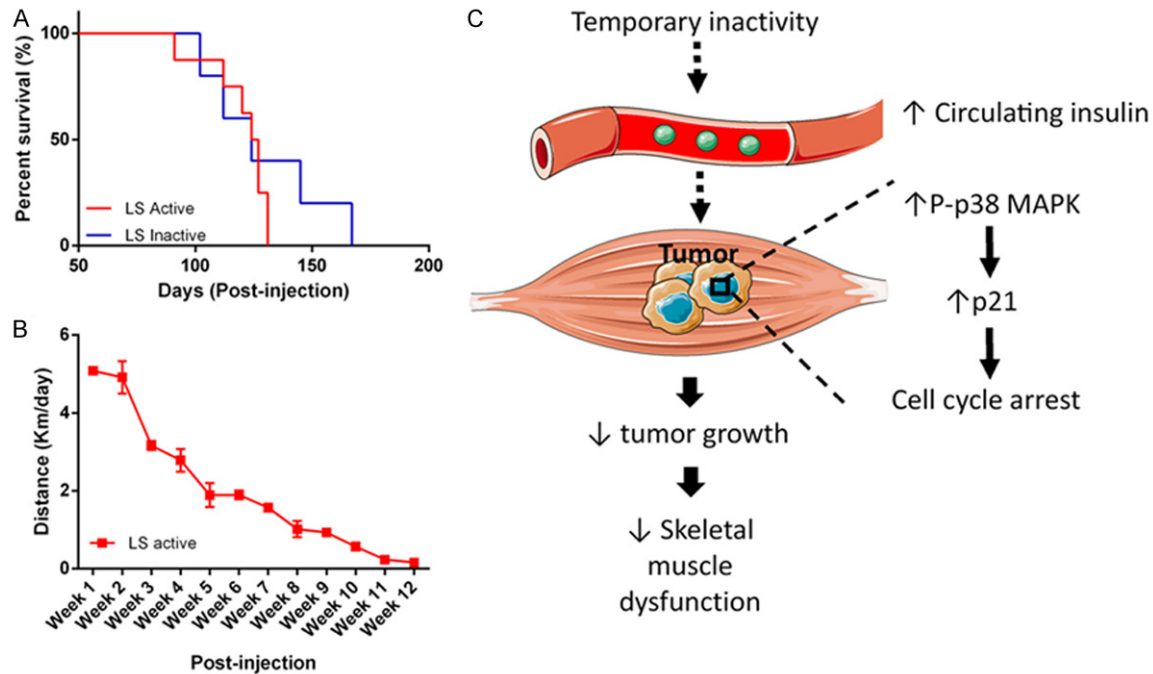
Figure 8. The impact of PA levels on overall mice lifespan. (A) Median of animal survival determined by the Kaplan-Meier method, results are expressed as the percentage of animal survival. (B) Week average of voluntary running distance per group (Km/day). Values were registered daily, until 12th week, the time at which LSA mice stopped activity on wheels. (C) Illustration showing a possible mechanism in which temporary physical inactivity could mediate the activation of p38 MAPK-p21 pathway, *via* insulin, within intramuscular tumor to limit its growth and reduce skeletal muscle dysfunction.

Interestingly, insulin also significantly up-regulated p21 mRNA expression at 1 h PT ($P = 0.02$) and, then, p21 protein content starting from 2 h PT (**Figure 7A** and **7B**) with a statistical significance reached at 4 h PT (+36%, $P = 0.02$; **Figure 7C** and **7D**). Afterward, we determined if the expression of p21 was regulated by p38; thus, we inhibited the activity of p38 MAPK with a specific chemical inhibitor, SB203508, before exposing cells to insulin. We observed that in the presence of insulin, blocking p38 downstream cascade resulted in a clear decrease in p21 mRNA (1.62 ± 0.3 vs. 0.79 ± 0.2, $P = 0.01$; **Figure 7F**) and protein expression compared to cells treated with insulin alone (-53.6%, $P < 0.001$; **Figure 7G** and **7H**). Our results demonstrate that the expression of p21 was, at least, partly regulated by p38 MAPK in response to insulin treatment. These *in vitro* findings may comfort our *in vivo* data and, therefore, suggest that insulin could be potentially responsible for the activation of p38 and p21 expression in LS tumors. These events were probably behind

the reduced tumor growth seen in inactive animals.

PA did not significantly affect survival in SW872 tumor-bearing mice

We finally studied the impact of tumor burden on overall survival. Mice that died before the development of obvious intramuscular tumor were excluded from the protocol. At 19th week of the survival protocol, 100% of active mice died compared to 60% of mortality in the inactive group. Although inactive mice showed a tendency to live longer, this did not reach any statistical difference (**Figure 8A**). The median survival was ~120 days for active mice and 130 days for inactive mice. Given the bulky size of tumor, LSA mice became totally inactive at the 12th week (**Figure 8B**), which probably decreased the severity of the disease and, thus, restrained the difference in term of survival between both groups. However, given the few number of inactive mice included in the survival curve, the impact of PA on overall lifes-

pan deserves to be addressed in the future using a larger number of mice.

Discussion

Data describing the impact of PA on sarcoma growth are scarce and almost inexistent. A previous study showed that BDF1 mice bearing subcutaneous S-180 sarcoma cells and undergoing a continuous swimming training, before and after inoculation, exhibited a reduced tumor volume [23]. Contrary to this study, we found that LS within skeletal muscle developed faster in response to voluntary PA. At the end of the protocol, tumor weight was ~1.5 fold higher in the active group and coincided with greater cellular mitosis and proliferation, as evidenced by a higher mitotic index and Ki-67 staining on tumor sections. In line with this enhancement of tumor mass, muscle strength and endurance running capacity were weakened earlier in active mice. These observations were probably not the result of muscle atrophy, since skeletal muscle weights remained unchanged. The localization of LS within lower limbs confers it the particularity of being in direct interaction with muscle; thus, we suppose that the rapid development of LS in active mice constituted a bulging mass that aggravated skeletal muscle dysfunction.

Based on these data and our findings that intratumor angiogenesis and pro-apoptotic pathways were not affected by PA, it seems that tumor proliferation was the main mechanism modulated in response to regular PA. MAPKs are well-known to control cell proliferation, differentiation, senescence and apoptosis [13]. A previous report has identified a role for the JNK-downstream, c-jun, in promoting intramuscular LS progression in mice bearing SW872 tumor [24]. In the present study, only p38 MAPK was activated in response to the drop in PA levels; $p38^{Thr180/Tyr182}$ was barely phosphorylated in tumor of active mice, while its phosphorylation increased dramatically in the inactive group. The activation of p38 in animals exhibiting reduced tumor growth may indicate an eventual anti-oncogenic property. The role of p38 as a tumor suppressor has been extensively discussed previously and seems to be cell-context and cell-type specific [25, 26]; p38 exerts its suppressive function by up-regulating the expression, stabilizing the protein structure

and directly activating a number of factors involved in cell cycle arrest such as p21, 27 and 53 [27, 28]. Accordingly, the expression of p21, but not of p27, at both mRNA and protein level was increased in tumors of inactive animals. Indeed, p38 can directly interact with p53 and induce its phosphorylation on the ser^{15} residue [27], activated p53 is then able to translocate into nucleus to induce the expression of *p21* [28]. However, in our study the transcriptional activation of *p21* was p53-independent, since SW872 cells may express a decoy form of p53 with single-mutation isoleucine-to-asparagine at the 251 codon [29]. The unmodulated expression of *p16^{INK4}* and *p14^{ARF}* as well as hallmarks of heterochromatin structure such as trimethyl lysine 9 of histone 3 (H3K9me3) (data not shown), suggest that senescence-like growth arrest is unlikely to occur. It appears that p21-mediated cell cycle blockade was the main event responsible for delaying tumor growth in inactive animals.

Various cellular stimuli may induce the activation of p38 and downstream cascade. Insulin has been described as a possible activator for p38 signaling [30]. Interestingly, the circulating amounts of insulin and the activation of related pathways are highly influenced by the levels of PA [22]. For example, 11-week of physical inactivity, by wheel lock, significantly increased the levels of circulating insulin in tumor-bearing mice [31]. Accordingly, we found that basal levels of insulin were 4 fold higher in inactive compared to active tumor-bearing mice. The values of insulin were within range comparing to previous studies performed on non-fasting tumor-bearing mice, suggesting that our inactive mice exhibited moderate insulin rates and were less likely to develop hyperinsulinemia or insulin-resistance [32, 33]. Insulin up-regulated the expression of p21 at the mRNA and protein level in a p38-dependent manner, since the inhibition of p38 activity with SB203580 abolished the increase of p21 in SW872 tumor cells. The evidence that p38 controls p21 expression was also unveiled in prostate, lung and breast cancer cells using SB203580 [34-36]. Even in highly proliferative Ras-transformed myoblast cells, insulin blocked cell cycle and induced differentiation through reactivating p38 [37]. Thus, the antimitotic properties of insulin could be driven by its capacity to pro-

mote cell cycle blockade prior to differentiation. Insulin was able to reduce growth and promote differentiation in LS cell lines such as, Lisa-2, MLS-402 and MLS-1765 [38, 39]. Cavin proteins that stabilize insulin signaling were more expressed in the least aggressive well-differentiated LS tumors [38]. Accordingly, Codenotti and colleagues proposed that a decrease in insulin signaling may promote LS progression and dedifferentiation [38]. These observations together with the present results may shed light about a possible role for insulin in delaying LS growth and aggressiveness. Although high amounts of insulin have been linked to tumor cell survival and growth [40], moderate levels could produce the opposite effects in adipocytic tumors that are particularly sensitive to insulin-induced differentiation mechanisms [41, 42]. Adipocytes, the cell origin of LS, mostly express the insulin receptor (IR)-B isoform [43], which is specific for insulin [44] and predominantly induces metabolic signals, cell cycle withdrawal and differentiation [45]. Whereas, the IR-A isoform that binds both insulin and insulin-like growth factor II (IGF-II) [44] is mainly associated with proliferation and anti-apoptotic responses and is mostly expressed in brain, spleen and prostate [46, 47]. Altogether, insulin induces differential signaling in a tissue-dependent manner and, therefore, the impact of insulin on LS, suggested in this study, is specific for tumors from adipocytic origin.

As depicted in **Figure 8C**, we suppose that a temporary period of inactivity may induce a moderate but sufficient increase in circulating insulin levels that could act on intramuscular tumor and activate p38 MAPK. Then, p38 upregulates the expression of p21, which in turn can block cell cycle and delay tumor growth. Our findings are with high translational relevance. Indeed, patients with lower-extremities LS usually undergo a preoperative period in which they receive neoadjuvant anticancer therapies in order to shrink tumor and make limb-spared surgery more feasible [48]. To date, there is no information about the levels of PA to recommend for those patients. Our study may suggest that reducing the levels of PA could be advised for patients waiting for surgery, especially those who were highly active before diagnosis of cancer. A future retrospective study is planned to investigate the impact of PA levels practiced by each patient, before/

after diagnosis of lower-limbs LS, on tumor stage and the expression status of p21.

Disclosure of conflict of interest

None.

Address correspondence to: Dr. Amélie Rébillard, EA1274 Laboratory "Movement, Sport and Health Sciences" M2S, University of Rennes 2-ENS Rennes, Bruz 35170, France. Tel: (33) (0)2 90 09 15 87; E-mail: amelie.rebillard@univ-rennes2.fr

References

[1] Courneya KS and Friedenreich CM. Physical activity and cancer: an introduction. Recent Results Cancer Res 2011; 186: 1-10.

[2] Battaglini C, Bottaro M, Dennehy C, Rae L, Shields E, Kirk D and Hackney AC. The effects of an individualized exercise intervention on body composition in breast cancer patients undergoing treatment. Sao Paulo Med J 2007; 125: 22-28.

[3] Lynch BM, Neilson HK and Friedenreich CM. Physical activity and breast cancer prevention. Recent Results Cancer Res 2011; 186: 13-42.

[4] Ballard-Barbash R, Friedenreich CM, Courneya KS, Siddiqi SM, McTiernan A and Alfano CM. Physical activity, biomarkers, and disease outcomes in cancer survivors: a systematic review. J Natl Cancer Inst 2012; 104: 815-840.

[5] Meyerhardt JA, Heseltine D, Niedzwiecki D, Hollis D, Saltz LB, Mayer RJ, Thomas J, Nelson H, Whittom R, Hantel A, Schilsky RL and Fuchs CS. Impact of physical activity on cancer recurrence and survival in patients with stage III colon cancer: findings from CALGB 89803. J Clin Oncol 2006; 24: 3535-3541.

[6] Friedenreich CM, Neilson HK, Farris MS and Courneya KS. Physical activity and cancer outcomes: a precision medicine approach. Clin Cancer Res 2016; 22: 4766-4775.

[7] Ashcraft KA, Peace RM, Betof AS, Dewhirst MW and Jones LW. Efficacy and mechanisms

of aerobic exercise on cancer initiation, progression, and metastasis: a critical systematic review of in vivo preclinical data. Cancer Res 2016; 76: 4032-4050.

[8] Sim FH, Frassica FJ and Frassica DA. Soft-tissue tumors: diagnosis, evaluation, and management. J Am Acad Orthop Surg 1994; 2: 202-211.

[9] Peterson JJ, Kransdorf MJ, Bancroft LW and O'Connor MI. Malignant fatty tumors: classification, clinical course, imaging appearance and treatment. Skeletal Radiol 2003; 32: 493-503.

[10] Wampler MA, Galantino ML, Huang S, Gilchrist LS, Marchese VG, Morris GS, Scalzitti DA, Hudson MM, Oeffinger KC, Stovall M, Leisenring WM, Armstrong GT, Robison LL and Ness KK. Physical activity among adult survivors of childhood lower-extremity sarcoma. J Cancer Surviv 2012; 6: 45-53.

[11] McTiernan A. Mechanisms linking physical activity with cancer. Nat Rev Cancer 2008; 8: 205-211.

[12] Jones LW, Antonelli J, Masko EM, Broadwater G, Lascola CD, Fels D, Dewhirst MW, Dyck JR, Nagendran J, Flores CT, Betof AS, Nelson ER, Pollak M, Dash RC, Young ME and Freedland SJ. Exercise modulation of the host-tumor interaction in an orthotopic model of murine prostate cancer. J Appl Physiol (1985) 2012; 113: 263-272.

[13] Dhillon AS, Hagan S, Rath O and Kolch W. MAP kinase signalling pathways in cancer. Oncogene 2007; 26: 3279-3290.

[14] Pedersen L, Idorn M, Olofsson GH, Lauenborg B, Nookaew I, Hansen RH, Johannesen HH, Becker JC, Pedersen KS, Dethlefsen C, Nielsen J, Gehl J, Pedersen BK, Thor Straten P and Hojman P. Voluntary running suppresses tumor growth through epinephrine- and IL-6-dependent NK cell mobilization and redistribution. Cell Metab 2016; 23: 554-562.

[15] Betof AS, Lascola CD, Weitzel D, Landon C, Scarbrough PM, Devi GR, Palmer G, Jones LW and Dewhirst MW. Modulation of murine breast tumor vascularity, hypoxia and chemotherapeutic response by exercise. J Natl Cancer Inst 2015; 107.

[16] Ray MA, Trammell RA, Verhulst S, Ran S and Toth LA. Development of a mouse model for assessing fatigue during chemotherapy. Comp Med 2011; 61: 119-130.

[17] Assi M, Derbre F, Lefeuvre-Orfila L and Rebillard A. Antioxidant supplementation accelerates cachexia development by promoting tumor growth in C26 tumor-bearing mice. Free Radic Biol Med 2016; 91: 204-214.

[18] Vakkila J and Lotze MT. Inflammation and necrosis promote tumour growth. Nat Rev Immunol 2004; 4: 641-648.

[19] Schieven GL. The biology of p38 kinase: a central role in inflammation. Curr Top Med Chem 2005; 5: 921-928.

[20] Wood CD, Thornton TM, Sabio G, Davis RA and Rincon M. Nuclear localization of p38 MAPK in response to DNA damage. Int J Biol Sci 2009; 5: 428-437.

[21] Sato A, Okada M, Shibuya K, Watanabe E, Seino S, Narita Y, Shibui S, Kayama T and Kitanaka C. Pivotal role for ROS activation of p38 MAPK in the control of differentiation and tumor-initiating capacity of glioma-initiating cells. Stem Cell Res 2014; 12: 119-131.

[22] Balkau B, Mhamdi L, Oppert JM, Nolan J, Golay A, Porcellati F, Laakso M, Ferrannini E; EGIR-RISC Study Group. Physical activity and insulin sensitivity: the RISC study. Diabetes 2008; 57: 2613-2618.

[23] Sasvari M, Taylor AW, Gaal D and Radak Z. The effect of regular exercise on development of sarcoma tumor and oxidative damage in mice liver. J Sports Sci Med 2011; 10: 93-96.

[24] Dass CR, Galloway SJ, Clark JC, Khachigian LM and Choong PF. Involvement of c-jun in human liposarcoma growth: supporting data from clinical immunohistochemistry and DNAzyme efficacy. Cancer Biol Ther 2008; 7: 1297-1301.

[25] Bulavin DV and Fornace AJ Jr. p38 MAP kinase's emerging role as a tumor suppressor. Adv Cancer Res 2004; 92: 95-118.

[26] Han J and Sun P. The pathways to tumor suppression via route p38. Trends Biochem Sci 2007; 32: 364-371.

[27] Lee YJ, Kuo HC, Chu CY, Wang CJ, Lin WC and Tseng TH. Involvement of tumor suppressor protein p53 and p38 MAPK in caffeic acid phenethyl ester-induced apoptosis of C6 glioma cells. Biochem Pharmacol 2003; 66: 2281-2289.

[28] Sun YW, Herzog CR, Krzeminski J, Amin S, Perdew G and El-Bayoumy K. Effects of the environmental mammary carcinogen 6-nitrochrysene on p53 and p21(Cip1) protein expression and cell cycle regulation in MCF-7 and MCF-10A cells. Chem Biol Interact 2007; 170: 31-39.

[29] Forbes S, Clements J, Dawson E, Bamford S, Webb T, Dogan A, Flanagan A, Teague J, Wooster R, Futreal PA and Stratton MR. Cosmic 2005. Br J Cancer 2006; 94: 318-322.

[30] Igarashi M, Yamaguchi H, Hirata A, Daimon M, Tominaga M and Kato T. Insulin activates p38 mitogen-activated protein (MAP) kinase via a MAP kinase kinase (MKK) 3/MKK 6 pathway in vascular smooth muscle cells. Eur J Clin Invest 2000; 30: 668-677.

[31] Yan L and Demars LC. Effects of non-motorized voluntary running on experimental and spontaneous metastasis in mice. Anticancer Res 2011; 31: 3337-3344.

[32] Asp ML, Tian M, Wendel AA and Belury MA. Evidence for the contribution of insulin resistance to the development of cachexia in tumor-bearing mice. Int J Cancer 2010; 126: 756-763.

[33] Zhu Z, Jiang W, McGinley JN and Thompson HJ. Energetics and mammary carcinogenesis: effects of moderate-intensity running and energy intake on cellular processes and molecular mechanisms in rats. J Appl Physiol (1985) 2009; 106: 911-918.

[34] Gan L, Wang J, Xu H and Yang X. Resistance to docetaxel-induced apoptosis in prostate cancer cells by p38/p53/p21 signaling. Prostate 2011; 71: 1158-1166.

[35] Zhou Y, Tang Q, Zhao S, Zhang F, Li L, Wu W, Wang Z and Hann S. Targeting signal transducer and activator of transcription 3 contributes to the solamargine-inhibited growth and -induced apoptosis of human lung cancer cells. Tumour Biol 2014; 35: 8169-8178.

[36] Kang N, Wang MM, Wang YH, Zhang ZN, Cao HR, Lv YH, Yang Y, Fan PH, Qiu F and Gao XM. Tetrahydrocurcumin induces G2/M cell cycle arrest and apoptosis involving p38 MAPK activation in human breast cancer cells. Food Chem Toxicol 2014; 67: 193-200.

[37] Conejo R, de Alvaro C, Benito M, Cuadrado A and Lorenzo M. Insulin restores differentiation of Ras-transformed C2C12 myoblasts by inducing NF-kappaB through an AKT/P70S6K/p38-MAPK pathway. Oncogene 2002; 21: 3739-3753.

[38] Codenotti S, Vezzoli M, Poliani PL, Cominelli M, Bono F, Kabbout H, Faggi F, Chiarelli N, Colombi M, Zanella I, Biasiotto G, Montanelli A, Caimi L, Monti E and Fanzani A. Caveolin-1, caveolin-2 and cavin-1 are strong predictors of adipogenic differentiation in human tumors and cell lines of liposarcoma. Eur J Cell Biol 2016; 95: 252-264.

[39] Wabitsch M, Bruderlein S, Melzner I, Braun M, Mechtersheimer G and Moller P. LiSa-2, a novel human liposarcoma cell line with a high capacity for terminal adipose differentiation. Int J Cancer 2000; 88: 889-894.

[40] Zhang H, Fagan DH, Zeng X, Freeman KT, Sachdev D and Yee D. Inhibition of cancer cell proliferation and metastasis by insulin receptor downregulation. Oncogene 2010; 29: 2517-2527.

[41] Font de Mora J, Porras A, Ahn N and Santos E. Mitogen-activated protein kinase activation is not necessary for, but antagonizes, 3T3-L1 adipocytic differentiation. Mol Cell Biol 1997; 17: 6068-6075.

[42] Mariani O, Brennetot C, Coindre JM, Gruel N, Ganem C, Delattre O, Stern MH and Aurias A. JUN oncogene amplification and overexpression block adipocytic differentiation in highly aggressive sarcomas. Cancer Cell 2007; 11: 361-374.

[43] Serrano R, Villar M, Martinez C, Carrascosa JM, Gallardo N and Andres A. Differential gene expression of insulin receptor isoforms A and B and insulin receptor substrates 1, 2 and 3 in rat tissues: modulation by aging and differentiation in rat adipose tissue. J Mol Endocrinol 2005; 34: 153-161.

[44] Belfiore A, Frasca F, Pandini G, Sciacca L and Vigneri R. Insulin receptor isoforms and insulin receptor/insulin-like growth factor receptor hybrids in physiology and disease. Endocr Rev 2009; 30: 586-623.

[45] Sciacca L, Prisco M, Wu A, Belfiore A, Vigneri R and Baserga R. Signaling differences from the A and B isoforms of the insulin receptor (IR) in 32D cells in the presence or absence of IR substrate-1. Endocrinology 2003; 144: 2650-2658.

[46] Vienberg SG, Bouman SD, Sorensen H, Stidsen CE, Kjeldsen T, Glendorf T, Sorensen AR, Olsen GS, Andersen B and Nishimura E. Receptor-isoform-selective insulin analogues give tissue-preferential effects. Biochem J 2011; 440: 301-308.

[47] Perks CM, Zielinska HA, Wang J, Jarrett C, Frankow A, Ladomery MR, Bahl A, Rhodes A, Oxley J and Holly JM. Insulin receptor isoform variations in prostate cancer cells. Front Endocrinol (Lausanne) 2016; 7: 132.

[48] Goss G and Demetri G. Medical management of unresectable, recurrent low-grade retroperitoneal liposarcoma: integration of cytotoxic and non-cytotoxic therapies into multimodality care. Surg Oncol 2000; 9: 53-59.